High Power Test of a SLED System with Dual Side-Wall Coupling Irises for Linear Colliders

Hiroshi Matsumoto, Hiroshi Baba, Atsushi Miura and Seiya Yamaguchi
KEK, National Laboratory for High Energy Physics
Oho 1-1, Tsukuba-shi, Ibaraki-ken 305, Japan

Abstract

A new SLED cavity has been developed for the 1.54 GeV injector linac of the KEK Accelerator Test Facility (ATF). A significant reduction of electric fields near the irises has been achieved by adopting dual side-wall coupling irises. The new SLED cavities were successfully operated at an output rf-power of 380 MW after the total operation time of 500 hours without any serious breakdown problems.

I. INTRODUCTION

The Japan Linear Collider (JLC) [1] aims to deliver electron-positron collisions at a center-of-mass energy of 300~500 GeV with a luminosity of ~ 5×10^{33} $cm^{-2}s^{-1}$. The KEK Accelerator Test Facility (ATF) [2] is presently under construction as a test facility for the JLC. The ATF consists of a 1.54 GeV S-band injector linac and a 1.54 GeV test damping ring.

To meet the energy goal 1.54 GeV of the injector linac with a given site constraint the accelerating gradient has to reach 33 MV/m. The mission of SLED cavities is to deliver the required 400 MW output power with an 85 MW input from the klystron. The regular unit of the linac consists of two 3 m-long accelerating structures, an 85 MW klystron with a SLED and a klystron modulator. High power (85 MW) klystron with 4.5 μs pulse width have been developed by TOSHIBA corporation and available since 1989 [3].

The original SLED [4] scheme has been used extensively and reliably at SLAC for the SLC over the past several years. At the SLC the klystron output power is 65 MW with a pulse width 3.5 μs. The achieved peak power, after the pulse compression, is 300 MW. The maximum power from SLED in practice could be limited by the rf breakdown around the irises due to the high surface electric field [5] . At the ATF the input rf-power will be 85 MW, well above the SLC SLED case. An excessive surface field within the cavity leads to potentially serious breakdown problems and radiation safety hazards. Thus a care must be taken to reduce the surface field around the irises. We have found that adopting two port side-wall coupling irises is a good solution for this problem.

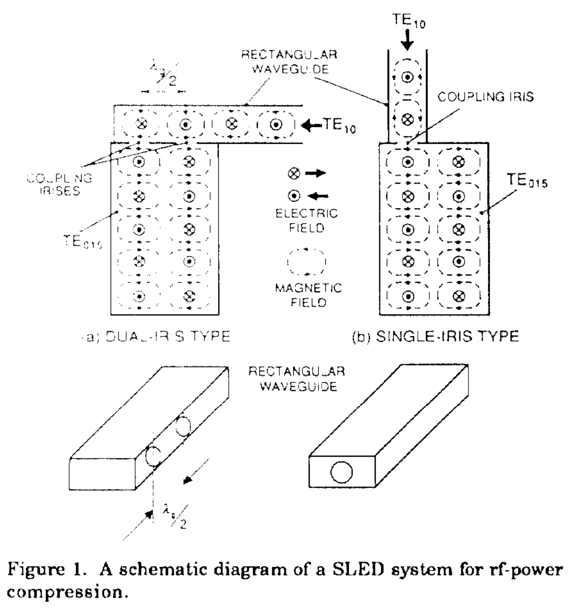

Figure 1. A schematic diagram of a SLED system for rf-power compression.

II. DESIGN AND FABRICATION OF THE SLED

Figure 1 shows a schematic diagram of the dual-iris (new) and single-iris (original) SLED systems. Important design principles of the dual-iris SLED system are: (1) implement two irises for the rf-coupling, (2) the coupling is made on the side wall of the wave guide so as to reduce the surface electric field, and (3) adopt a sturdy mechanical structure for operational stability.

A. *Main Parameters of SLED*

Parameters of the present SLED cavity such as Q_0 and β have been chosen so as to achieve a maximum energy gain of the accelerating structures for the ATF with an input rf-power of 85 MW and pulse width of 4.5 μs [3, 6]. They are summarized in Table 1.

Table 1
Main parameters of the dual-iris SLED system.

Operation frequency		2856	MHz
Cavity size	: length (L)	33.59	cm
	: Diameter ($2a$)	20.51	cm
Groove size	: Width (w_g)	1.0	cm
	: Depth (d_g)	0.9	cm
Iris size	: Diameter (D)	2.98	cm
	: Thickness (t_w)	1.2	cm
Quality factor (Q)		$\sim10^5$	
Coupling coefficient (β)		4.8	
SLED filling time, $T_c = 2Q_0 / w(1+\beta)$		1.92	μs
Klystron pulse width (t)		4.5	μs
SLED output pulse width		1.0	μs
Mode separation between TE_{015} and TM_{115}		20	MHz
Structure	: Length	3	m
	: Attenuation parameter (τ)	0.57	
Filling time		0.83	μs

B. *Coupling Irises*

The surface electric field E that appears around the coupling iris is qualitatively written as

$$E \propto \frac{\sqrt{P}}{D}\ , \qquad (1)$$

where P is the power transmitted through the iris and D is the iris diameter. Here we evaluate the benefits of a dual-iris structure compared to a single-iris scheme. We use suffixes 1 and 2 to denote the parameters in a single-iris and dual-iris cases. We assume that the allowed surface field strength E is limited by breakdown conditions. Therefore, the maximum E should be limited at the same value, independent of the iris scheme choice. Thus we set $E_1 = E_2 = E$. It follows that

$$\frac{\sqrt{P_1}}{D_1} = \frac{\sqrt{P_2}}{D_2}. \qquad (2)$$

Hence,

$$\frac{2P_2}{P_1} = \frac{2D_2^2}{D_1^2}. \qquad (3)$$

The coupling coefficients per iris for both type cavities are

$$\beta_1 = 2\beta_2 \qquad (4)$$

Here the β is known to be proportional to D^6 in an ideally simplified case. If the power loss in the cavity and the wave guide can be neglected, the β is also proportional to the coupling magnetic field [7, p. 143-149]. Thus we get

0-7803-1203-1/93$03.00 © 1993 IEEE

$$D_1^6 = 2D_2^6. \quad (5)$$

We apply the relation (5) in the equation (3) to obtain:

$$\frac{2P_2}{P_1} = \frac{2D_2^2}{(2^{1/6}D_2)^2} = 1.59. \quad (6)$$

This means that the excitation of the dual-iris SLED cavity can be 1.59 times that of the original single-iris cavity. This gain can be further increased by building irises on the side wall of the wave guides, rather than having them on the end wall, as shown in Figure. 1. This is because the electric field strength on the side wall of the wave guide near the iris is smaller than the maximum transverse electric field in the wave guide which appears when the rf-power propagates. In the case of the S-band rectangular wave-guide (72.1 mm × 34.0 mm) , their ratio λ_c/λ_g is 0.924, where λ_c and λ_g are the cutoff- and guide-wavelength. Therefore, the equation (5) can be modified as

$$D_1^6 = (0.924)^2 \times 2D_2^6 = 1.71 D_2^6. \quad (7)$$

By using the equation (7), instead of (5), in (3) we obtain

$$\frac{2P_2}{P_1} = \frac{2D_2^2}{(1.71^{1/6}D_2)^2} = 1.67. \quad (8)$$

By adopting dual side-wall irises, the transmitted power into the SLED cavity can be increased by a factor 1.67, while maintaining the same iris surface field.

In the discussion above the wall thickness at the irises and the power loss on the copper surface have been neglected. Because of their effects in a real SLED cavity a small correction needs to be applied to the expected ratio $2P_1/2P_{2I}$ in equation (8).

C. Design of the S-band SLED Cavity

To determine optimum cavity dimensions such as the radius (a) and length (L), we have taken a procedure as follows:

(1) Calculate various modes and obtain the optimum $Q \cdot (\delta/\lambda)$ as function of $2a/L$, where δ is the skin depth. The a and L are searched for in a reasonable range for fabrication.
(2) Evaluate the mechanical stability for the preferred $2a/L$
(3) Examine the distribution of neighboring modes and the electromagnetic fields.

At SLAC the TE_{015} mode has been chosen from considerations on cost, mechanical stability and mode separation [8]. The SLAC decision has a proven performance record. We have taken the same choice. The degeneracy of TM_{115} and TE_{015} modes can be removed by introducing a circular groove on the end plate of the cavity. The URMEL code [9] was used to calculate the resonant frequencies of the two modes as functions of the groove width (w_g) and depth (d_g). The resonant frequency of the TM_{115} mode is always decreased by introducing a groove. Considering the high Q value of the TE_{015} mode, the dimension of the groove was chosen to be w_g = 10 mm and d_g= 9 mm, which gives a mode separation of 20 MHz.

D. Three Dimensional Calculations with MAFIA

Having confirmed the principle of a dual-iris scheme with a cold model, we have carried out three dimensional (3D) field calculations using the MAFIA code [10]. The goal was to find the geometry that minimizes the electric fields at the irises. Figure 3 shows the electromagnetic fields for both SLED schemes. It can be seen that the two irises in the dual-iris SLED scheme [11] are excited at opposite phases. This means that the TM_{115} mode is hard to be excited at this frequency. By adding the effect of the groove discussed in the pervious section to this fact, the dual-iris SLED cavity is completely free from the TM_{115} mode at this frequency.

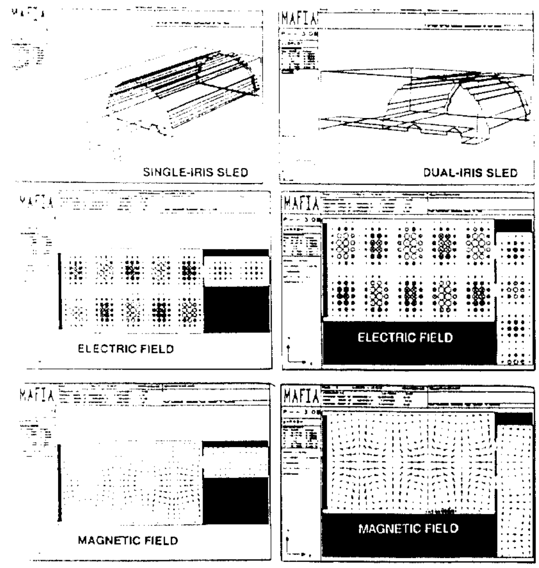

Figure 3. Electromagnetic fields in the SLED cavities calculated by MAFIA code.

The relationship between the coupling coefficient β and the iris diameter D has been calculated in two steps. In the first step the external Q value of the coupling iris (Q_{ext}) was determined by using the "Tuning Method" developed by J.C. Slater [7, p. 87]. In the second step the β was calculated from the relationship $\beta = Q_0/Q_{ext}$. Figure 4 shows the measured and calculated relationship between β and D of our dual-iris SLED cavities for the varying iris thickness obtained by using a cold model. The results are plotted for several different iris thickness t_w.

The agreement between the calculations and measurements is quite good. The combination of the Tuning Method and 3D calculations with MAFIA turns out very useful in design work of SLED cavities. In the dual-iris scheme SLED cavity it has been shown that β is proportional to $D^{8.4}$ and $\exp(-0.224 t_w)$. It is seen that the iris surface field can be reduced by increasing D and t_w.

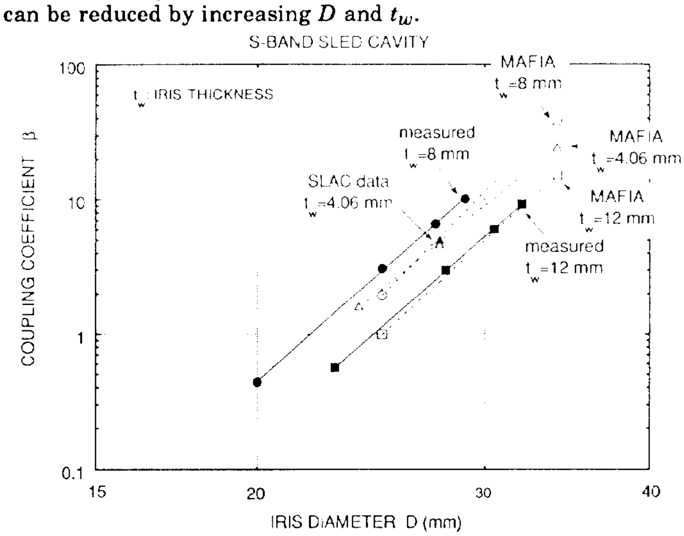

Figure 4. Calculated and measured β values as a function of iris diameter and thickness.

E. Mechanical Structure and Fabrication of the Cavities

Figure 5 shows a photograph of the present dual-iris S-band SLED system. A part of the end wall of the cavity was machined to form a thin area so that the position of the end wall can be moved with a differential screw which is attached on an external jig. This allows a frequency tuning of ±1 MHz.

A copper cooling water pipe was welded to the cylinder wall and the grooves were formed on the outside of the end walls as a cooling water channel. The positions of water pipes were chosen to match the wall current pattern of the TE_{015} mode for efficient cooling.

The two cavities were held within four thick plates (3 cm) of stainless steel. These plates were connected with each other by four pipes of stainless steel which were also used as headers of the cooling water system. Since this support structure is an integral part of the cooling system, the temperature difference between the cavity and the support is minimized. Because of this rigid and stable support system, these SLED cavities can be used even in a free posture.

The cavity material is class 2 OFHC which has been delivered by Hitachi Densen Corp. The machining of the cavity surface was made with an accuracy of ± 5 μm and the surface roughness < 0.2 μm. The Q_0 has been measured to be the order of 10^5.

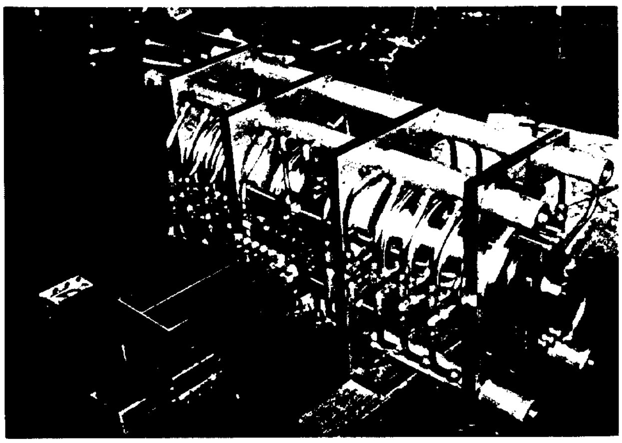

Figure 5. A photograph of the present dual-iris SLED system.

III. EXPERIMENTAL SETUP AND PROCEDURE

The final goal of the present experiment is to demonstrate the peak power of ~400 MW with the pulse compression for the KEK ATF. Experimental set up consists of an 85 MW klystron system, the SLED cavities, high power wave-guides, rf-loads and a vacuum pump system. To absorb the high peak power (~ 400 MW) from the SLED cavities, four dummy loads are used. They have been developed at SLAC for use with 100 MW power with 1 μs pulse length at 30 pps repetition rate. The phase reversal response time of the circuit is less than 40 ns [13, 14]. The base vacuum pressure of 6×10^{-9} Torr was achieved by using three ion pumps.

The rf processing was carried out while monitoring the vacuum pressure and the rf power levels from various spots in the system. The characteristic time constants in this procedure are determined empirically, and are incorporated in the computer control program.

IV. EXPERIMENTAL RESULTS

The rf processing of the wave guide and the rf loads were first carried out by detuning the SLED cavities by up to 75 MW with a full-length 4.5 μs pulse. Then the cavities were tuned to the operation frequency and the rf processing was applied again until the input power is increased to 80 MW. This was done without using phase reversing. At this stage the peak output power from the SLED cavities was 2.2 times the input power.

After the pre-processing, SLED operations with rf phase switching were started, first at a low rf power level. The resonant frequency of the cavities was measured during the rf processing from time to time. It was confirmed that the mechanical structure of the SLED cavity was very stable, and a re-tuning of the cavities was not necessary after the initial low rf power turning. During the rf processing the vacuum pressure was maintained below 5×10^{-8} Torr and the reflecting rf-power less than 1 MW.

After the total operation time of 500 hours, the input power was increased up to 80 MW with 4.5 μs pulse width. The peak output power 380 MW was achieved as shown in Figure 6. The maximum X-ray intensity measured on the irises was 4.8 mR/h during the whole process of the operation.

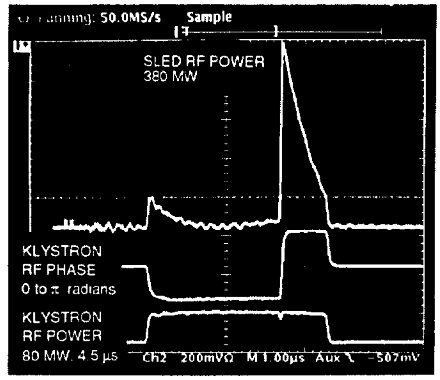

Figure 6. A photograph of the wave forms of input (lower) and output (upper) rf-power of SLED system and phase of the input rf signal (middle) .

V. ACKNOWLEDGMENTS

The authors wish to thank Professors Y. Kimura and K. Takata of KEK for their continuous encouragement. The present work has been carried out as part of the construction program of the KEK ATF, collaboration by: S. Takeda, M. Akemoto, H. Hayano, T. Naito, Y. Otake, J. Urakawa, and others too numerous to list at KEK, and T. Matsui and S. Morita of ATC Corp. Their help is greatly appreciated. The authors are grateful for critical reading of the manuscript by N. Toge, M. Yoshioka and T. Shintake. A special mention has to be made that the present work could not have been carried out without many discussions with and information from Professor G. A. Loew, Mrs. Z. D. Farkas, R. Forks, H. Deruyter and their colleagues at SLAC. Their generosity in sharing their expert knowledge is greatly acknowledged.

VI. REFERENCES

[1] JLC group, KEK report 92-16, A/H/M, National Laboratory for High Energy Physics, Japan, December 1992.
[2] S. Takeda, Proc. of the Second Workshop on Japan Linear Collider (JLC), KEK, 1990, p. 6~17.
[3] H. Yonezawa, S. Miyake, K. Gonpei, K. Ohya and T. Okamoto, Proc. 14th Int. Conf. on High Energy Accelerators, Tuskuba, JAPAN, 1989, p. [1177]/219-224.
[4] P. B. Wilson, SLAC-TN-73-15, 1973.
[5] G. A. Loew, Private discussion for the present status of SLAC SLED system, SLAC, 1990.
[6] Z. D. Farkas, H. A. Hogg, G. A. Loew and P.B. Wilson, Proc. 9th Int. Conf. on High Energy Accelerators, SLAC, 1974, p. 576.
[7] J. C. Slater, "Microwave Electronics", D. Van Nostrand Company Inc., p. 87, p. 143~149.
[8] Z. D. Farkas, H. A. Hogg, G. A. Loew and P.B. Wilson, SLAC-PUB-1561, March 1975
[9] T. Weiland, Nucl. Inst. Meth. 216 (1983), p. 329 - 348
[10] M. Bartsch, M. Dehler, M. Dohlus, P. Hahne, R. Klatt, F. Krawcyzk, Z. Min, T. Pröpper, P. Schütt, T. Weiland, S. Wipf, M. Marx, F. Ebeling and B. Steffen, Proc. 1990 Linac Conference, Albuquerque, 1990, p. 372~377.
[11] A. Fiebig, R. Hohbach, P. Marchand and J. O. Pearce, CERN/PS 87-45 [RF], March 1987.
[13] Heinz D. Schwarz, SLAC-PUB-3600, March 1985.
[14] S. Araki and Y. Otake, Proc. of the 16th Linear Accelerator Meeting in Japan. September 3~5, 1991, p. 97~99.